Proceedings of the 4th International Conference on Functional Materials and Civil Engineering
DOI: 10.54254/2755-2721/2026.36565

Tin Metasurface-Based Visible-Light Absorber

Fanru Sun

School of Electronic and Optical Engineering, Nanjing University of Science and Technology, Nanjing, China
19550090706@163.com

Abstract. To achieve efficient absorption of the visible spectrum, this work presents a three-layer metasurface visible-light absorber based on a metal-insulator-metal (MIM) stacked structure, with titanium nitride (TiN) employed as the top-layer material in place of the conventional noble metal.The absorber adopts gold (Au) as the substrate material, silicon dioxide (SiO_2) as the intermediate dielectric layer, and the top-layer TiN pattern is designed as irregular polygonal columnar structures.Simulation calculations are performed to evaluate the absorption performance and electric field distribution. The results indicate that the proposed absorber achieves an average absorptivity of 94.83% over the 300-1000 nm wavelength range. Combined with the analysis of the electric field distribution maps, it is revealed that the top layer of the structure supports both localized surface plasmon resonance (LSPR) and Fabry–Pérot (FP) cavity resonance. This synergistic effect enables an absorptivity exceeding 95% across the 671-1000 nm band, with a peak value of 99.88% near 739 nm, thereby realizing perfect absorption.

Keywords: metasurface, visible-light absorber, titanium nitride (TiN)

1. Introduction

Metasurfaces are a class of two-dimensional planar structures belonging to the family of metamaterials [1]. Composed of periodically arranged subwavelength artificial unit cells, they can overcome the limitations of conventional materials in terms of volume, functionality, and other aspects [2-4]. Among them, metasurface absorbers (MSAs) have attracted considerable attention [5, 6]. Currently, visible-light metasurface absorbers still suffer from two major shortcomings: in terms of materials, the conventional metals used as the absorbing medium are costly and exhibit poor thermal stability; in terms of structure, most designs adopt hollow-shell models or ultra-multilayer stacks, which are not amenable to large-scale fabrication.

To address the above issues, this paper proposes a novel visible-light metasurface absorber based on a three-layer Au-SiO-TiN structure. Distinct from existing absorber designs, the top layer innovatively employs an irregular columnar pattern incorporating corner cutting, elliptical holes, and other geometric elements to achieve perfect absorption in the 300-1000 nm wavelength range. Using the finite element method, this work focuses on investigating its absorption characteristics, electric field distribution, and the underlying physical mechanisms, as well as exploring the influence of geometric parameters on the spectral absorption performance.

© 2026 The Authors. This is an open access article distributed under the terms of the Creative Commons Attribution License 4.0 (https://creativecommons.org/licenses/by/4.0/).

DOI: 10.54254/2755-2721/2026.36565

2. Structural design

The solar absorber proposed in this work follows the classic metal–insulator–metal three-layer nanoarray structure, but replaces the conventional noble metal in the top resonant elements with titanium nitride (TiN) ceramic, as shown in Figure 1. From bottom to top, a gold (Au) reflective layer suppresses transmission; a silicon dioxide (SiO_2) layer with a refractive index of 1.45 serves as the dielectric spacer and provides a propagation channel for electromagnetic waves; and the top layer consists of an array of irregular polygonal pillars made of TiN, as illustrated in Figure 1(b). The period of the unit cell is p, and the thicknesses of the individual layers are h_1,h_2 and h_3. The basic shape of the top TiN pattern is a square with side length w_1. Asymmetric modifications are applied to the unit cell to introduce multiple geometric degrees of freedom: three of its corners are truncated by a quarter-circle of radius w_2, while the remaining corner is cut out by a square notch of side length w_2. At the center of the unit cell, two concentric elliptical holes are placed, with semi-axes (a_1,b_1) and (b_1,a_1) arranged orthogonally to each other, as shown in Figure 1(c). The values of the relevant parameters are summarized in Table 1.This asymmetric, multi-scale geometric design of the top layer aims to introduce rich plasmon hybridization modes [7], effectively broadening the absorption bandwidth of the absorber through electromagnetic coupling among multiple resonant elements across a wide spectral range.

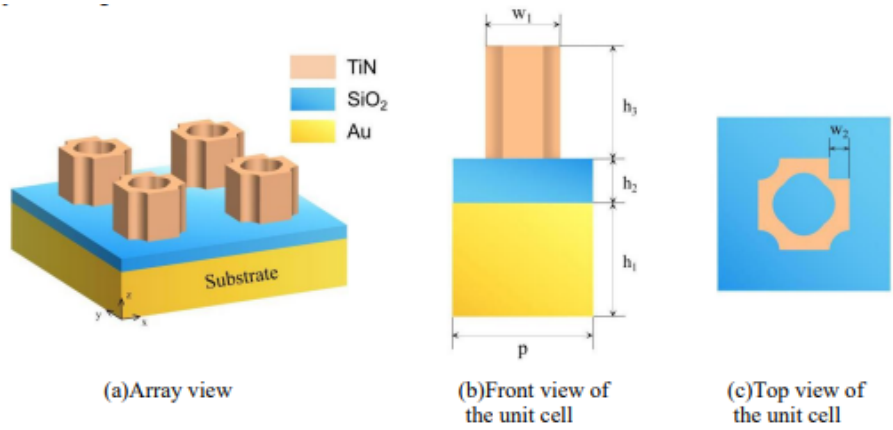


Figure 1. Schematic of the absorber

Table 1. Physical parameters of the proposed absorb

Parameter	Value/nm	Parameter	Value/nm
h_1	400	w_1	230
h_2	110	w_2	60
h_3	400	a_1	65
p	500	b_1	55

Figure 2 shows a schematic illustration of the fabrication process of the solar absorber.The silicon substrate was sequentially cleaned by ultrasonication in acetone and deionized water. Then, Au and SiO_2thin films were successively deposited by magnetron sputtering to serve as the back reflector layer and the dielectric spacer layer, respectively. The top TiN irregular polygonal columnar patterns were fabricated using ultraviolet (UV) lithography combined with a lift-off process. Specifically, a

DOI: 10.54254/2755-2721/2026.36565

photoresist was uniformly spin-coated onto the SiO_2 surface, followed by pre-baking, selective UV exposure, developing, and hard-baking, yielding a photoresist mask complementary to the target pattern. Subsequently, a TiN thin film was deposited using the same magnetron sputtering parameters as those for the bottom layers. Finally, the photoresist was removed with acetone, resulting in a periodic array of irregular TiN columnar structures.

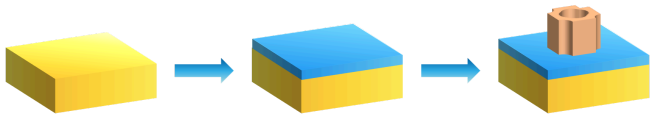


Figure 2. Schematic of the fabrication process

3. Result and analysis

In this study, the optical performance of the absorber was numerically simulated using COMSOL software based on the finite element method (FEM). In the simulation, the incident light source was set as a plane wave with a wavelength range of 300 nm to 1000 nm. Perfectly matched layers (PMLs) were applied in the z-direction to eliminate errors caused by non-physical reflections from the computational boundaries [8-10]. Periodic boundary conditions were imposed in the x and y directions. Reflectance and transmittance monitors were placed above the irregular TiN columnar array and below the Au substrate, respectively. Since the thickness of the Au reflecting bottom layer is much greater than the skin depth of the incident light, the transmittance (T) is approximately zero [11-14]. Consequently, the absorptance can be calculated as:

$$A = 1 - R \tag{1}$$

where A refers to the absorptance and R refers to the reflectance [11-14].

3.1. Absorption performance

The proposed absorber exhibits an average absorptivity of 94.83% over the wavelength range of 300-1000 nm, essentially achieving perfect absorption, with its absorption spectrum shown in Figure 3. The absorptivity remains consistently above 95% in the 671-1000 nm band, a phenomenon attributed to the asymmetry of the top-layer pattern. Four distinct absorption peaks are observed in the spectrum, and their corresponding absorptivity values are listed in Table 2.

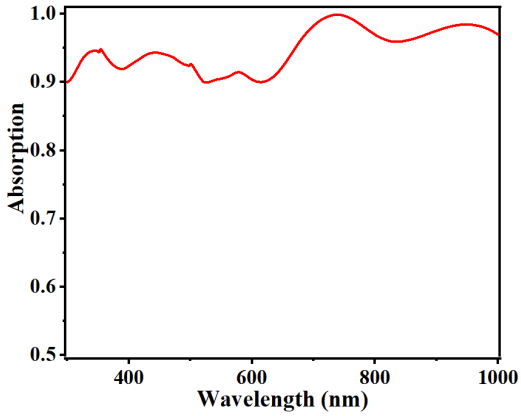


Figure 3. Absorption spectrum of the metasurface

DOI: 10.54254/2755-2721/2026.36565

Table 2. Absorption peaks and their corresponding wavelengths

Wavelength/nm	Absorption	Wavelength/nm	Absorption
345	94.62%	739	99.88%
442	94.33%	947	98.45%

3.2. Absorption mechanism

Localized surface plasmon resonance (LSPR) phenomena are observed on both sides of the irregular TiN unit structures, as shown in Figure 4. By comparing Figure 4(a) and (b), it is found that near λ = 945 nm, the electric field distribution further penetrates into the SiO_2 dielectric layer. This observation indicates that strong coupling occurs between the LSPR mode of the top TiN layer and the Fabry–Pérot (FP) cavity resonance [15] formed by the Au/SiO_2/TiN structure, giving rise to a hybrid LSPR-FP resonant mode.

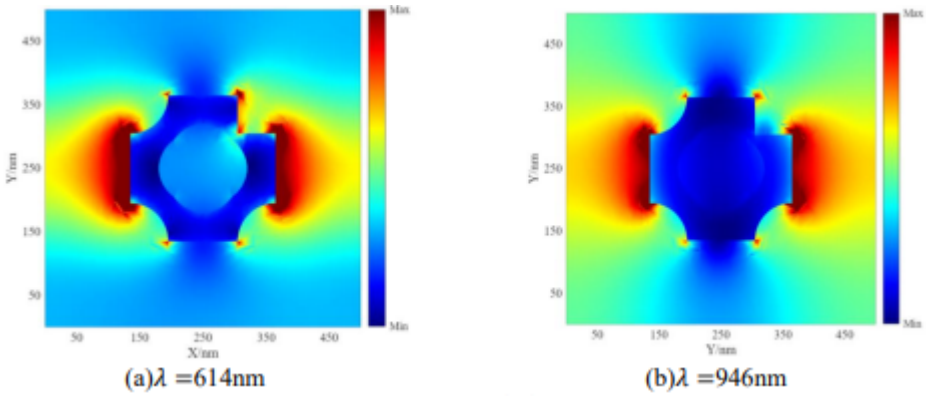


Figure 4. Electric field $|E|$ distribution

3.3. Influence of structural parameters on absorption performance

In this paper, the control variable method is employed to analyze the absorption performance of the device by varying the top-layer TiN thickness h_3 and the unit-cell feature width w_1 individually, while keeping other parameters fixed. Table 3 lists the average absorptivity of the device for different values of h_3 and w_1.

Table 3. Average absorption versus structural parameters

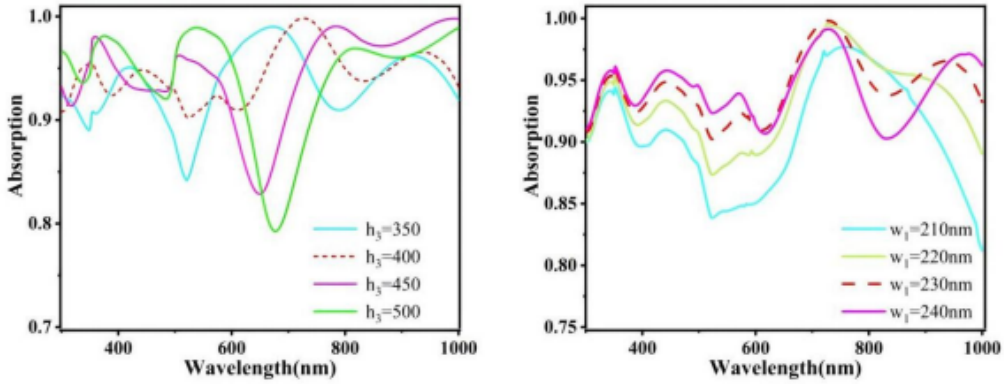
h_3/nm	Average absorption	w_1/nm	Average absorption
350	93.51%	210	90.65%
400	94.50%	220	93.36%
739	94.57%	230	94.50%
947	94.06%	240	94.31%

Figure 5 shows the influence of structural parameters on absorption.As shown in Figure 5(a), the highest average absorptivity is achieved at h_3=450 nm; however, the absorption spectrum exhibits a notable absorption dip near λ = 640 nm. At h_3= 400 nm, the average absorptivity is only 0.07%

DOI: 10.54254/2755-2721/2026.36565

lower than the maximum value, while the absorption spectrum is more stable. Consequently, h_3= 230 nm is determined as the optimal thickness. As depicted in Figure 5(b), the average absorptivity reaches its peak at w_1=230 nm as the lateral dimension of the unit cell increases; further increasing the dimension to 240 nm leads to a slight decrease in the average absorptivity. Therefore, w_1=230 nm is chosen as the optimal width.

In summary of the above parameter analysis, the top-layer thickness h_3 primarily affects the coupling efficiency between the LSPR and FP cavity modes, while the unit feature width w_1 governs the peak position of the localized plasmon resonance. Together, they collectively regulate the effective superposition of electromagnetic resonances across the visible spectral range.



(a) Height of the TiN array layer, h_3 (b) Side length of the basic TiN square, w_1

Figure 5. Influence of structural parameters on the absorptance

4. Conclusions

The metasurface absorber designed in this paper replaces the conventional noble metals such as gold and silver in the top layer of the traditional metal-insulator-metal stacked configuration with titanium nitride (TiN). The top-layer TiN adopts irregular columnar structures to excite LSPR modes. The absorber achieves an average absorptivity of 94.83% over the 300-1000 nm wavelength range, realizing perfect absorption. The design introduces elements such as corner cutting and elliptical holes to form an asymmetric geometry, which leads to strong coupling between the LSPR modes and the Fabry–Pérot (FP) cavity resonance constituted by the Au/SiO_2/TiN structure. As a result, the absorptivity exceeds 95% in the 671-1000 nm band. The research in this paper will have broad application prospects in photovoltaic cells, ultra-sensitive optical sensors, radar shielding, and other directions.

References

[1] Hajian, H., Rukhlenko, I. D., Hanson, G. W., & Ozbay, E. (2022). Anisotropic absorber and tunable source of MIR radiation based on a black phosphorus-SiC metasurface. *Photonics and Nanostructures – Fundamentals and Applications*. 10.1016/j.photonics.2022.101020

[2] Xu, X., Li, C., Li, W., Feng, J., & Li, W.-Y. (2025). Molecular solar thermal energy storage devices: Toward a more sustainable future. *Energy & Environmental Science, 18*(20), 8990-9017. https://doi.org/10.1039/d5ee02556g

[3] Wang, C., Xu, Y., Xu, H., & Liu, J. (2025). Lightweight holographic near-eye display system with self-charging capability using solar energy. *Photonics Research, 13*(7), 1792-1799. https://doi.org/10.1364/PRJ.554523

[4] Xu, Y., Yang, Q., Ma, S., Zhang, Q., Jiang, M., Fu, B., Song, C., Shang, W., Tao, P., & Deng, T. (2026). High-temperature solar-thermal steam generation: Materials, system design and applications. *Energy & Environmental Science, 19*(9), 2746-2787. https://doi.org/10.1039/d6ee00346j

DOI: 10.54254/2755-2721/2026.36565

[5] Zhou, J., Liu, X., Zhang, H., et al. (2021). Cross-shaped titanium resonators based metasurface for ultra-broadband solar absorption. *IEEE Photonics Journal, 13*, 1-8. DOI:10.1109/JPHOT.2021.3052990
[6] Landy, N. I., Sajuyigbe, S., Mock, J. J., Smith, D. R., & Padilla, W. (2008). Perfect metamaterial absorber. *Physical Review Letters, 100*, 207402.
[7] Li, Y., Zhang, C. Z., Wu, X., Wang, X. Y., Xu, J., & Kan, C. X. (2026). Au-catalyzed monodisperse colloidal Cu nanorods with widely tunable surface plasmon resonance. *Chemical Communications, 62*(43), 10972-10976. https://doi.org/10.1039/d6cc01280a
[8] Huang, S., Wan, M., Sun, M., Wang, X., & Xu, B. (2026). An asymmetric GaAs nanocylinder quasi-BIC metasurface for dual narrowband high-Q perfect absorption in the near-infrared region. *Physical Chemistry Chemical Physics, 28*(17), 10749-10757. https://doi.org/10.1039/d5cp04946f
[9] Jiang, L., Yuan, C., Li, Z., et al. (2013). Multi-band and high-sensitivity perfect absorber based on monolayer graphene metamaterial. *Diamond and Related Materials, 56*, e277. 10.1016/j.diamond.2013.108227
[10] Zhong, Y. K., Fu, S. M., Huang, W., et al. (2017). Polarization-selective ultra-broadband superabsorber. *Optics Express, 25*(4), A124-A133. https://doi.org/10.1364/OE.25.00A124
[11] Wu, P. H., Zhang, C. F., Tang, Y. J., et al. (2020). A perfect absorber based on similar fabry-perot four-band in the visible range. *Nanomaterials, 10*(3), 488. https://doi.org/10.3390/nano10030488
[12] Kim, G., Kim, S., Kim, H., Lee, J., Badloe, T., & Rho, J. (2022). Metasurface-empowered spectral and spatial light modulation for disruptive holographic displays. *Nanoscale, 14*(12), 4380-4410. https://doi.org/10.1039/d1nr07909c
[13] Wang, Y., Zhang, X., Zhang, X., Zhou, T., Cui, Z., & Zhang, K. (2022). A novel terahertz metasurface based on a single-walled carbon nanotube film for sensing application. *Journal of Materials Chemistry A, 10*(4), 1780-1787. https://doi.org/10.1039/d1ta09396g
[14] Xu, M., Guo, L., Zhang, P., Qiu, Y., Li, Q., & Wang, J. (2022). Near-perfect spectrally-selective metasurface solar absorber based on tungsten octagonal prism array. *RSC Advances, 12*(26), 16823-16834. https://doi.org/10.1039/d2ra02802f
[15] Liu, X., Li, J., Zhao, R., Zhang, Y., & Dong, Y. (2023). Enhanced chirality in a dielectric metasurface without breaking symmetry. *Physical Chemistry Chemical Physics, 25*(3), 2050-2055. https://doi.org/10.1039/d2cp04833g